GENERAL DYNAMICS
General Atomic Division

GA-7874

AD 668845

GAMMA-RAY SHIELDING STUDIES

FINAL REPORT

This document has been approved for public release and sale; its distribution is unlimited

Gulf General Atomic
Incorporated

P. O. Box 608, San Diego, California 92112

March 17, 1967

Reproduced by the
CLEARINGHOUSE
for Federal Scientific & Technical
Information Springfield Va. 22151

UNCLASSIFIED

AD 668 845

GAMMA-RAY SHIELDING STUDIES

J. A. Lonergan, et al

Gulf General Atomic, Incorporated
San Diego, California

17 March 1967

Processed for . . .

DEFENSE DOCUMENTATION CENTER
DEFENSE SUPPLY AGENCY

CLEARINGHOUSE
FOR FEDERAL SCIENTIFIC AND TECHNICAL INFORMATION

U. S. DEPARTMENT OF COMMERCE / NATIONAL BUREAU OF STANDARDS / INSTITUTE FOR APPLIED TECHNOLOGY

GENERAL DYNAMICS
General Atomic Division
JOHN JAY HOPKINS LABORATORY FOR PURE AND APPLIED SCIENCE
P.O. Box 608, San Diego, California 92112

GA-7874

GAMMA-RAY SHIELDING STUDIES

FINAL REPORT

Work done by:

J. A. Lonergan
E. A. Beaver
J. Parez
D. F. Herring

Report written by:

J. A. Lonergan

Project 553
Contract No. N228(62479)70201
U. S. Naval Radiological Defense Laboratory

March 17, 1967

CONTENTS

FIGURES

FIGURES (Contd.)

ABSTRACT

A monoenergetic beam of gamma rays was used to study the deep penetration of 10-MeV gamma radiation in aluminum. Recently a positron annihilation system was developed at General Atomic for the purpose of making shielding measurements in the energy range from 5 to 30 MeV. A beam of positrons from the General Atomic linear accelerator is directed at a thin foil of beryllium. Some of the positrons annihilate in flight while passing through the foil, yielding photons along the beam axis having energies equal to the positron plus ~0.75 MeV. The bremsstrahlung produced by the positrons passing through the foil is assessed by passing a known number of electrons through the same foil and making an appropriate subtraction from the positron induced photons.

In the work reported here a 10-MeV beam of photons was directed perpendicularly at a six-in. thick slab of aluminum. This thickness corresponds to about 0.95 mean free paths for 10 MeV photons in aluminum. Pulse height spectra of gamma rays emerging from the slab were measured at three forward angles, viz., 0°, 15° and 30°. A 5-in. by 6-in. NaI crystal housed and collimated with lead was used to make these measurements. The detection system was off-gated except during the beam pulse to reduce background. The contributions to the spectra of Compton and multiple scatter events are compared with predictions based on a Monte Carlo calculation. The calculations agree with the experimental results within the uncertainties associated with the latter.

1. INTRODUCTION

This final report describes the work performed on the gamma-ray shielding studies for the U. S. Naval Radiological Defense Laboratory under Contract N228(62479)70201. The studies were initially to be performed over a period of three years; however, due to funding difficulties the contract was terminated after 16 months.

The program objective was to study the deep penetration of monoenergetic gamma rays in various materials. There exist several means of calculating this phenomenon, however, these calculations have not been checked in certain energy regions. In this program we proposed to check these calculations in the energy region around 10 MeV where isotopic sources are not available. We are able to do this because of the existence of a unique monoenergetic gamma-ray source in the LINAC Facility at General Atomic.

The deep penetration problem has been studied in this program by measuring the angular and energy distributions of gamma rays emerging from a slab of material upon which is incident a monoenergetic gamma-ray beam. The simple slab geometry was chosen to simplify the comparison of our experimental results with the calculated predictions. In anticipation of this program, General Atomic constructed a new experimental area at the Linear Accelerator Facility. This area, referred to as the High Resolution Port (HRP), has the advantages of being a very low background area and being accessible while the accelerator is operating. In the HRP a second positron annihilation system was constructed for producing monoenergetic gamma rays. The first, which was constructed at General Atomic several years ago, has been used extensively in photonuclear work. Because of the load on this apparatus, it was necessary to build another one. The new positron annihilation system is described in the following section.

After the positron annihilation system was constructed and the properties of the gamma-ray beam it produced had been carefully determined, it was then used to measure the response function of the gamma-ray detection system designed for the gamma-ray shielding program. The measured response function was sent to the Naval Radiological Defense Laboratory where it was incorporated into an unfolding code which has been developed there. After the response function was measured the first shielding studies were begun. A monoenergetic beam of 10 MeV photons was directed at an aluminum shield approximately one mean free path thick. The pulse height spectra of the outgoing gamma rays were measured at several angles to the beam axis. The data obtained were then unfolded and compared with Monte Carlo calculations made by Berger at NBS.[1] By making this comparison we were able to comment on the validity of Monte Carlo calculations for deep penetration of gamma rays.

2. POSITRON ANNIHILATION SYSTEM

The function of this system is to produce monoenergetic gamma rays by in-flight annihilation of positrons. Positrons are created by bombarding a high-Z target with electrons from the first section of the linear accelerator. The electrons make bremsstrahlung, which in turn will make positron-electron pairs. The positrons are then focused by a magnetic lens located directly behind the target. From the lens, the positrons enter the second section of the linear accelerator. By adjusting the phase of the rf power in this second section so that it differs by 180° from that of the first section, positrons can be accelerated through the section while the electrons are dissipated. In this manner a beam of positrons ranging in energy from approximately 5 MeV to 30 MeV can be obtained. The details of the General Atomic positron source have been described in an article by Sund, et al.[2] The positron beam is then transported by two 36° sector magnets into the High Resolution Port. Here the beam passes through a thin beryllium foil and is then deflected through an angle of 45° into a Faraday cup. The current incident on the Faraday cup is measured thus providing a direct monitor of the positron beam. Positron currents of the order of 10^{-10} amperes have been observed in the Faraday cup.

In passing through the thin beryllium foil a small percentage (approximately 0.1%) of the positron beam will annihilate in flight with electrons in the foil. The annihilation process yields two photons which are distributed isotropically in the center-of-mass reference frame of the positron-electron system. However, when one transforms the distribution of emergent photons from the center-of-mass reference frame to the laboratory reference frame, one finds that the photons emerge predominantly along the beam axis in the forward and backward directions. The photons emitted in the forward direction will have an energy of $\sim$0.75 MeV plus the kinetic energy of the incident positron. Photons emerging in the backward direction will have an energy of $\sim$0.25 MeV. Detailed calculations to determine the energy and flux distributions of outgoing photons as a function of angle have been carried out. The results of these calculations have been reported in the first quarterly report of this program.[3]

The thickness of the annihilation foil is limited by multiple scattering of the beam in the foil since the entire positron beam emerging from the foil must be collected in the Faraday cup. If the foil is too thick, a significant number of positrons will scatter away from the beam axis and strike the walls of the beam box. There they will annihilate and give off photons which will have energies ranging from approximately the total energy of the positron down to .511 keV. Since these photons will represent noise to the gamma-ray detector they are to be avoided. Also if the positron beam is widely scattered the charge collected in the Faraday cup becomes an inaccurate measure of the number of incident positrons. The maximum foil thickness which caused negligible scattering of the beam out of the Faraday cup was 0.004 in. for 10 MeV positrons. The energy lost by 10 MeV positrons passing through a foil of this thickness was approximately 30 keV. However, the positron beam transported into the HRP has an energy spread of approximately 2 percent or 200 keV for a 10 MeV positron beam. Thus, the spread in energy of the incident beam predominantly defines the spread in the energy of the annihilation photons.

The photon beam passes from the vacuum system through a thin, stainless steel window and is then collimated by a 24-in. lead collimator. The lead gamma-ray collimator located along the axis of the photon beam is designed so that lead inserts with various size openings can be placed into position. In the experiments to be described here an insert with a 1-in. diameter opening was used. This collimator defined a solid angle of 0.96×10^{-3} steradians subtended at the beryllium target. As can be seen from our calculation of the photon energy dependence on angle,[2] the energy spread in the outgoing photon beam across this solid angle is about 0.2 percent. This is a factor of 12 smaller than the spread due to the spread in the incident positron energy so that the angular spread does not seriously affect the energy spread.

The positron annihilation system is depicted in Fig. 1. The annihilation target assembly contains an insulated collimator. The beam size and location are determined by monitoring the charge on this collimator. This assembly also contains the annihilation target support that is designed so that three different beryllium foils and a no-target configuration can be rotated into the beam. Both the collimator and the foil supports are electrically driven and can be operated remotely from the data room. The dump magnet provides a maximum field of about 9,000 gauss. This is sufficient to deflect 64 MeV positrons into the Faraday cup. The cup itself is of sufficient size to collect 60 MeV positrons. The dumping magnetic field is reversible so that electrons can also be deflected into the Faraday cup.

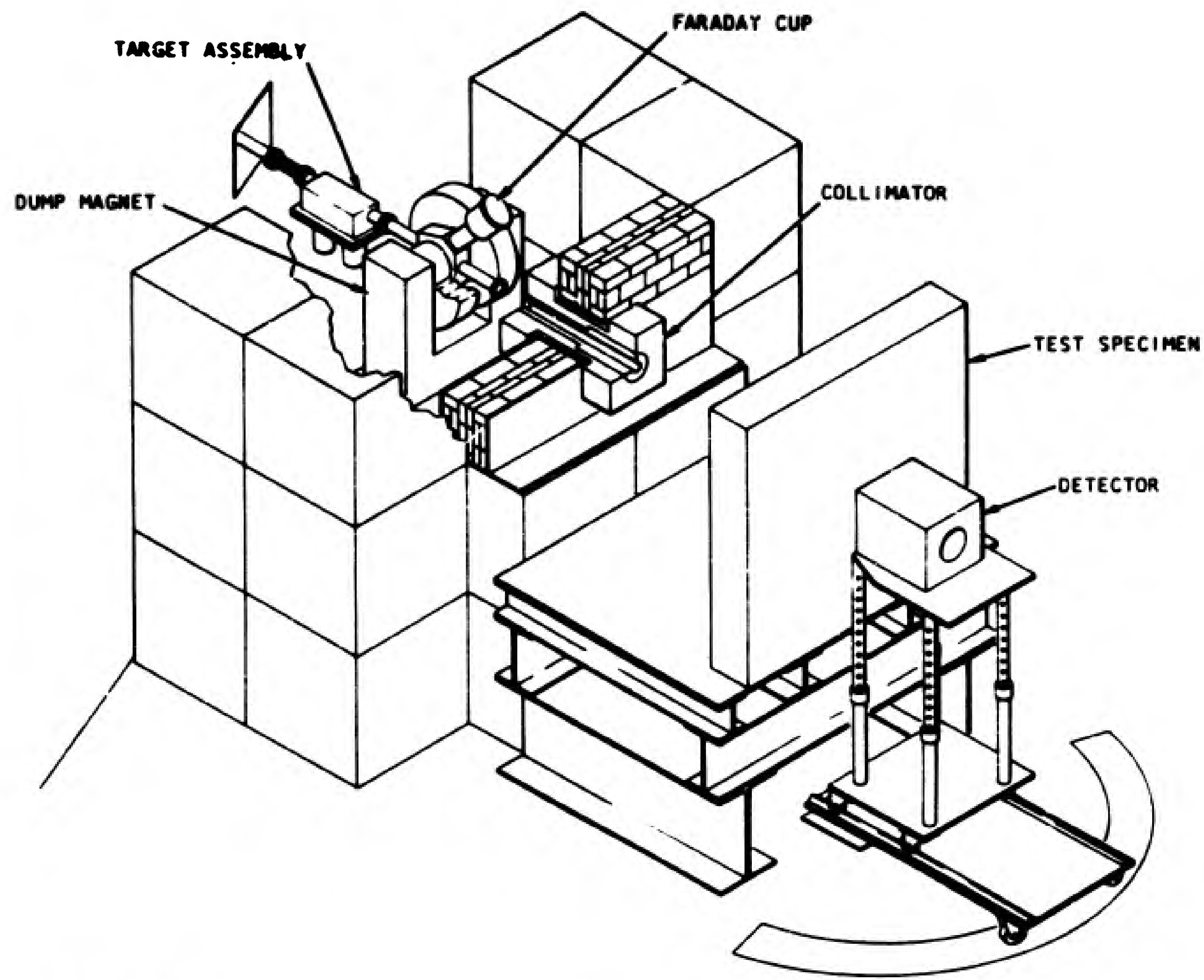

Fig. 1--Positron annihilation system and gamma-ray shielding apparatus

An example of gamma-ray pulse height spectra obtained with a 5 in. x 6 in. NaI crystal is shown in Fig. 2(a). The peak at the high energy end of the spectrum is due to the in-flight annihilation of positrons. The width is primarily determined by the resolution ($\sim$ 10 percent) of the detector. The energy spread of the beam, which is about 2 percent, is masked by the detector response. A large number of photons with energies below that corresponding to the annihilation peak are produced by the bremsstrahlung process as the positrons pass through the foil. The contribution to the total spectrum from bremsstrahlung has been reduced relative to the high energy photons by putting a beam hardener in the photon beam. In the experiments described here the hardener consisted of a 24-in. long graphite plug placed in the collimator. This hardener preferentially attenuates the low energy photons. The advantage of a higher annihilation-photon peak to bremsstrahlung ratio usually outweighs the loss in intensity inherent in the hardening process.

To accurately determine the number and pulse height distribution of photons that can be associated with bremsstrahlung, the procedure used to produce the photons from the positron annihilation is repeated with electrons. Electrons from the high-Z target are accelerated in the same manner as the positrons and are transported into the HRP where they pass through the beryllium foil and are collected in the Faraday cup. By collecting the same number of electrons as positrons the pulses due to bremsstrahlung can be determined. The small difference between the production of electron bremsstrahlung and positron bremsstrahlung occurs only at the very high energy end of the bremsstrahlung spectrum. At the energies that were used in this experiment neglecting the difference caused no significant error. An electron pulse height spectrum obtained in this manner is displayed in Fig. 2(b). The electron-induced spectrum is subtracted from the positron-induced spectrum to obtain the pulse height spectrum of photons

2a

2b

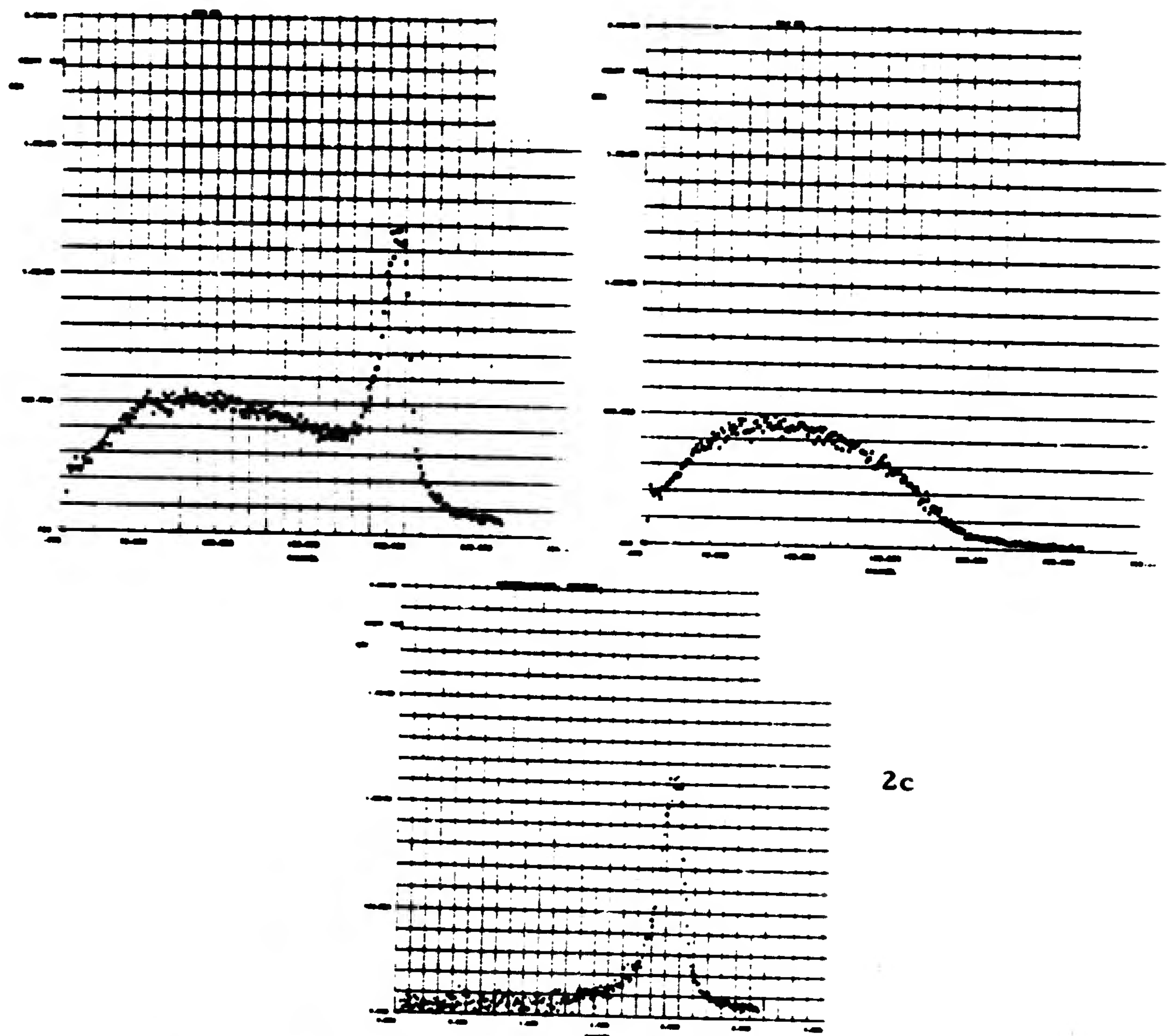

2c

Fig. 2a--Positron induced gamma-ray pulse height spectrum
2b--Electron induced gamma-ray pulse height spectrum
2c--Difference (β^+-e^-) gamma-ray pulse height spectrum.

from annihilation in-flight alone. Such a subtracted pulse height spectrum is shown in Fig. 2(c) and indeed a monoenergetic gamma ray is obtained.

The contamination of this beam due to scattering off various edges and components of the beam transport system was assessed by observing the photons coming from the annihilation system with no foil in place. A small number of counts was observed indicating that the contribution to the annihilation peak from undesired scattering or any other background source is < 1 percent.

The intensity of the monoenergetic photon beam can be determined from a knowledge of the incident positron current, the thickness of the annihilation foil, the solid angle defined by the collimator and subtended at the foil, and the cross section for in-flight annihilation. The cross section for in-flight annihilation has been calculated by Heitler.[4] His calculations have been checked at several energies by Seward, et al.,[5] and Kendall and Deutch.[6] The measurements have shown that the calculations of Heitler are correct to within the 10 percent experimental accuracy. However, it is expected that these calculations are more accurate than 10 percent and that our flux calculations are accurate to within a few percent. Typically, the monoenergetic gamma-ray beam intensity with a beam hardener in place is about 10^4 photons per sec at 10 MeV. The equation for photon flux is:

$$I\,(\text{photon/sec}) = \frac{i_+}{q}\ \eta\ t\ A \int_{\text{col}} \frac{d\sigma}{d\Omega}\ d\Omega \qquad (1)$$

In this equation i_+ is the positron current, q is the charge of a positron, η is the electron density in the foil, A is the attenuation due to the beam hardener, t is the thickness of the Be foil, and $\frac{d\sigma}{d\Omega}$ is the differential cross section for the in-flight annihilation of a positron with an electron. The integration is taken over the solid angle defined by the source collimator.

3. EXPERIMENTAL APPARATUS

The experimental apparatus is shown in Fig. 1 along with the positron annihilation system. The detector support and pig are also shown in the figure. The detector support table was constructed so that the detector could be rotated through an angle of 70° to the beam axis on both sides of that axis. The detector table itself can be varied in height so that measurements of gamma-ray spectra at various lateral distance from the beam axis can be made. A typical sample is also shown in Fig. 1. A plane view of the experimental arrangement is shown in Fig. 3, where the source collimator is shown on the left. An aluminum slab is located on the right along with the detector pig and collimator. The detector collimator has a 1-1/2-in. diameter opening at the entrance and a 3-in. diameter opening at the crystal. The detector pig was 3 in. thick at its thinnest point. The background observed in the detector during the runs was negligible. The pivot point of the rotating table is located on the beam axis at the exit surface of the slabs. The distance of the detector from the slab and the angle the detector axis makes with the beam axis were varied throughout the experiment, the specific values used are described in Section 5 along with the spectra observed. The detector itself was a 5 in. x 6 in. NaI crystal.

A block diagram of the electronic equipment which records and stores the gamma-ray pulses is given in Fig. 4. The function of this electronic system is to open the multichannel analyzer only when a beam pulse is on the foil and when the photon pulse corresponds to a gamma ray with energy greater than 0.30 MeV. By ignoring pulses that do not satisfy these criteria the background is greatly reduced. Also the system records the number of beam pulses incident on the target and the number of pulses associated with gamma rays. These two numbers can be quickly compared while the experiment is in progress in order to determine the extent of pile-up in the spectrum. Pile-up becomes important when the gamma-ray counting rate is more than a few percent of the beam pulse rate and the

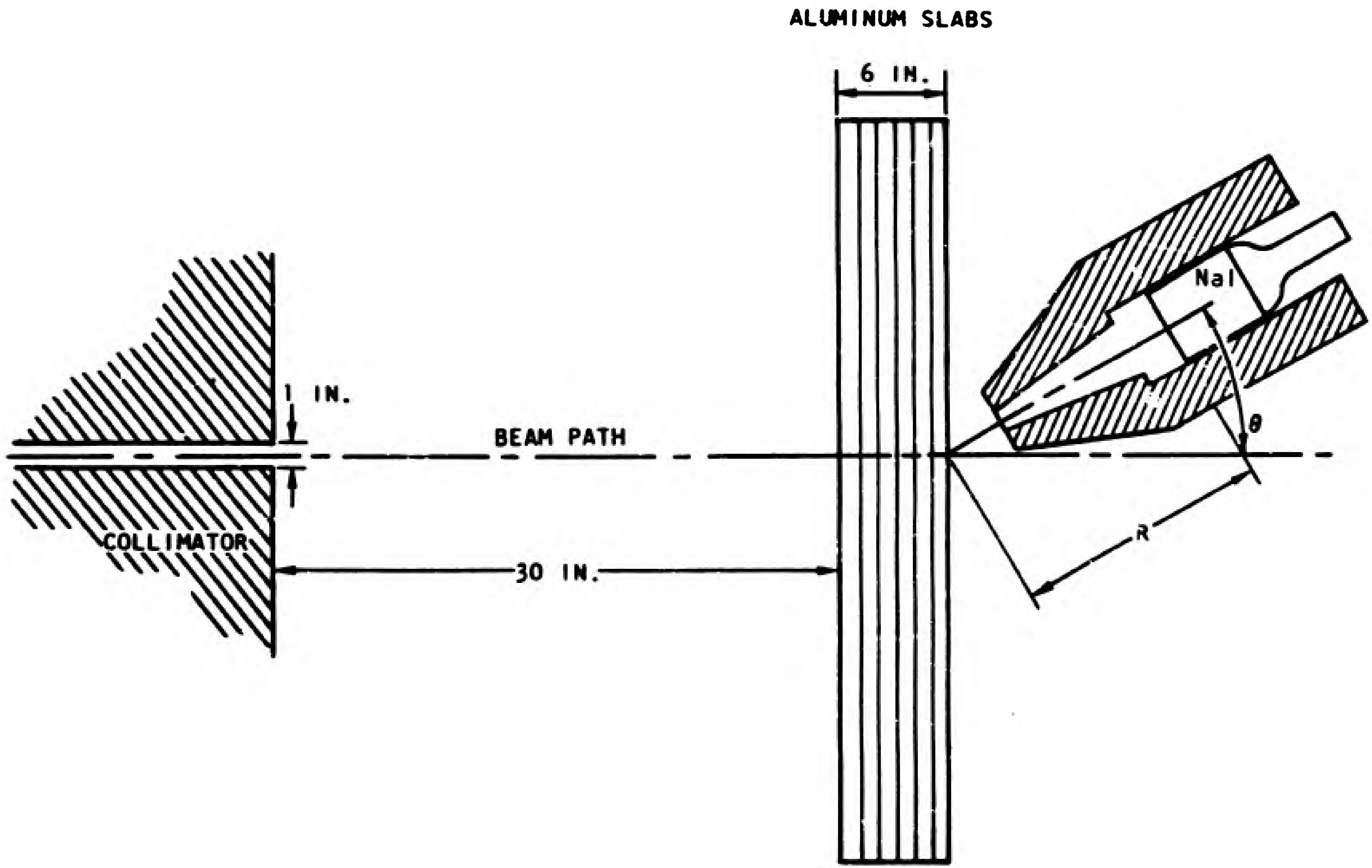

Fig. 3--Experimental arrangement

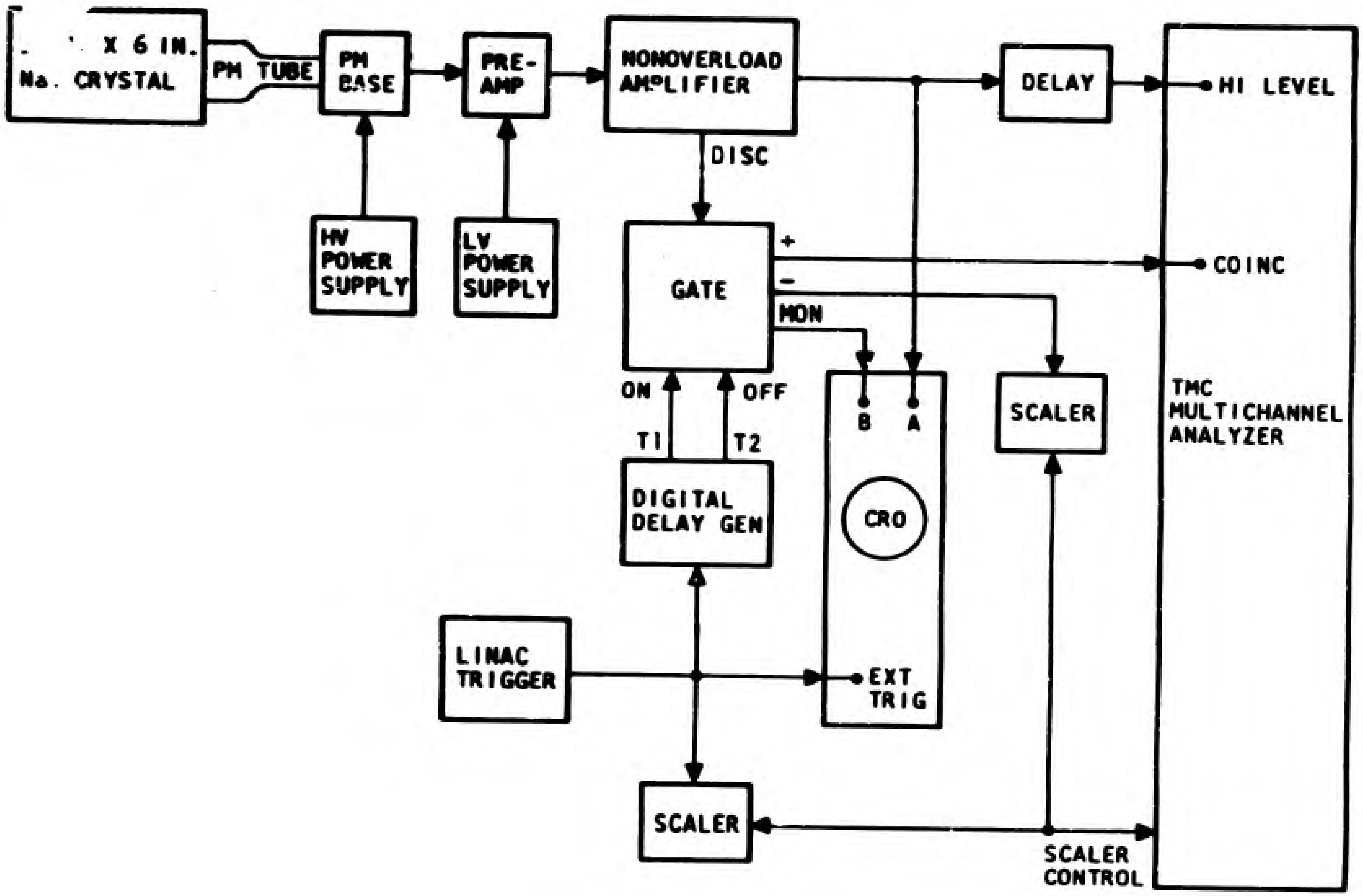

Fig. 4--Block diagram of the gamma-ray detection system

chance of obtaining two or more gamma rays during one beam pulse becomes significant. The positron beam current was always reduced to a level where the pile-up was less than one percent.

The number of photons incident on the target is determined from the number of positrons striking the beryllium foil which are in turn determined by measuring the charge collected in the Faraday cup. The system for measuring the charge collected is shown schematically in Fig. 5. The Faraday cup is connected directly by a short cable to a Keithley Model 418A picoammeter. This instrument, which is capable of measuring very low currents, has a zero to 3-volt output. A three-volt output corresponds to full scale deflection of the meter on the particular scale used. By placing this instrument in the High Resolution Port very close to the Faraday cup, it can be used as a preamplifier, thus eliminating the necessity of transferring a low level signal from the HRP to the data room. The high level signal from the picoammeter can be transferred to the data room without significant distortions due to noise pickup. In the data room the voltage output from the picoammeter is dropped across a precision resistor whose resistance is accurately known. The current passing through this resistor is then put into a current integrator. As can be seen from Fig. 5 the current integrator consists functionally of a capacitor upon which the charge is collected and across which the voltage is monitored. The charge collected on the Faraday cup can be computed with the following equation:

$$Q = \left[\frac{R}{v} \times I_f\right] \times CV \qquad (2)$$

where Q is the charge collected on the Faraday cup, R is the resistance of the precision resistor, v is the maximum output voltage of the picoammeter, I_f is the full-scale current reading of the particular scale to which the picoammeter is set, C is the capacitance of the capacitor upon which the charge is collected in the current integrator and V is the voltage read across the capacitor. Often when this arrangement is used, the voltage from the

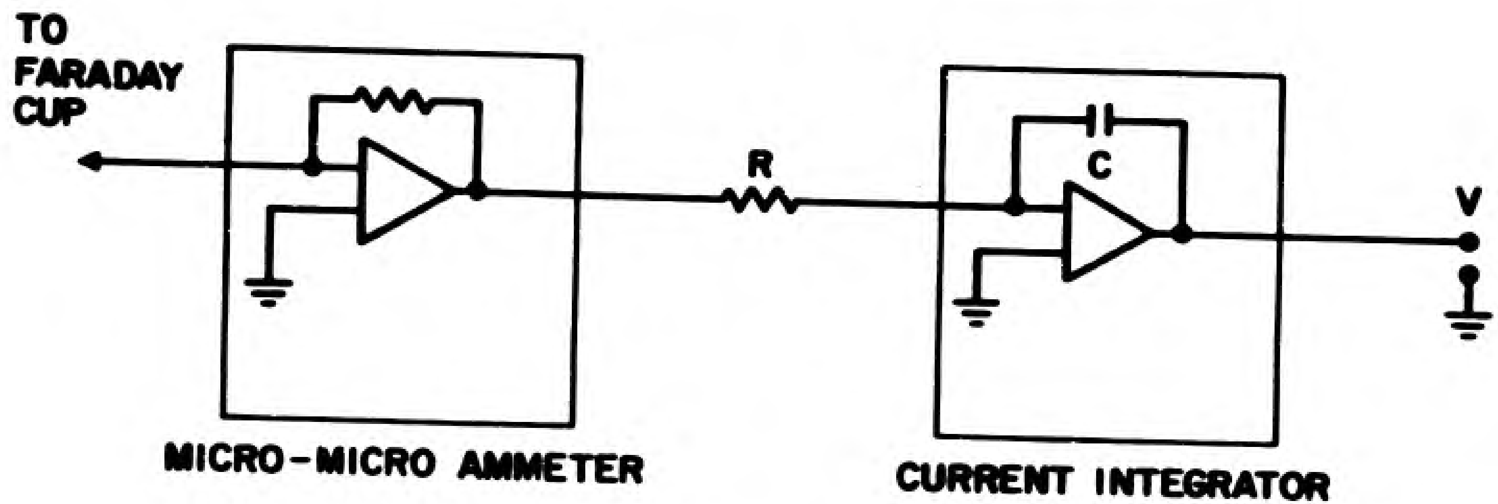

Fig. 5--Schematic diagram of the current integrating system

picoammeter is monitored independently with a voltmeter at a point between the precision resistor and the picoammeter. This voltage provides the LINAC operator with a means of monitoring the positron beam. The system has been calibrated by feeding an accurately known current into the input of the picoammeter and collecting the charge in the manner described. With this calibration the collected positron beam charge can be measured to within two percent.

4. RESPONSE FUNCTION

The first measurement that was made under this program determined experimentally the response function of the gamma-ray detection system. The monoenergetic gamma-ray beam from the positron annihilation system provides an ideal source for determining a response function. The energy spread of the photon beam is of the order of two percent and is much smaller than the response of the NaI crystal, which is expected to be of the order of 10 percent. The response function was determined by observing the pulse height spectrum produced by the monoenergetic gamma-ray beam. Sets of runs with positrons and electrons were made at various energies. The continuous contribution from the bremsstrahlung was determined and subtracted from each of the positron produced pulse height spectra. The subtraction was performed with the aid of a computer program which was written for this purpose. Examples of the different pulse height spectra taken at 10.84, 8.55 and 7.00 MeV are shown in Figs. 6, 7, 8. An attempt was made to obtain a spectrum from 4 MeV gamma rays. Although the beam was obtained at this energy, the positron current was too low to obtain statistically meaningful data. The experiment was repeated with a (Pu-Be) source which gives 4.43 MeV gamma rays. The background due to inelastic scattering of neutrons in the NaI crystal (which is considerable since (Pu-Be) is a neutron emitter) was reduced with paraffin and estimated by moving the detector out of the solid angle defined by the collimator of the positron annihilation system. In this position the gamma rays from the source, which was placed at the foil position, were attenuated

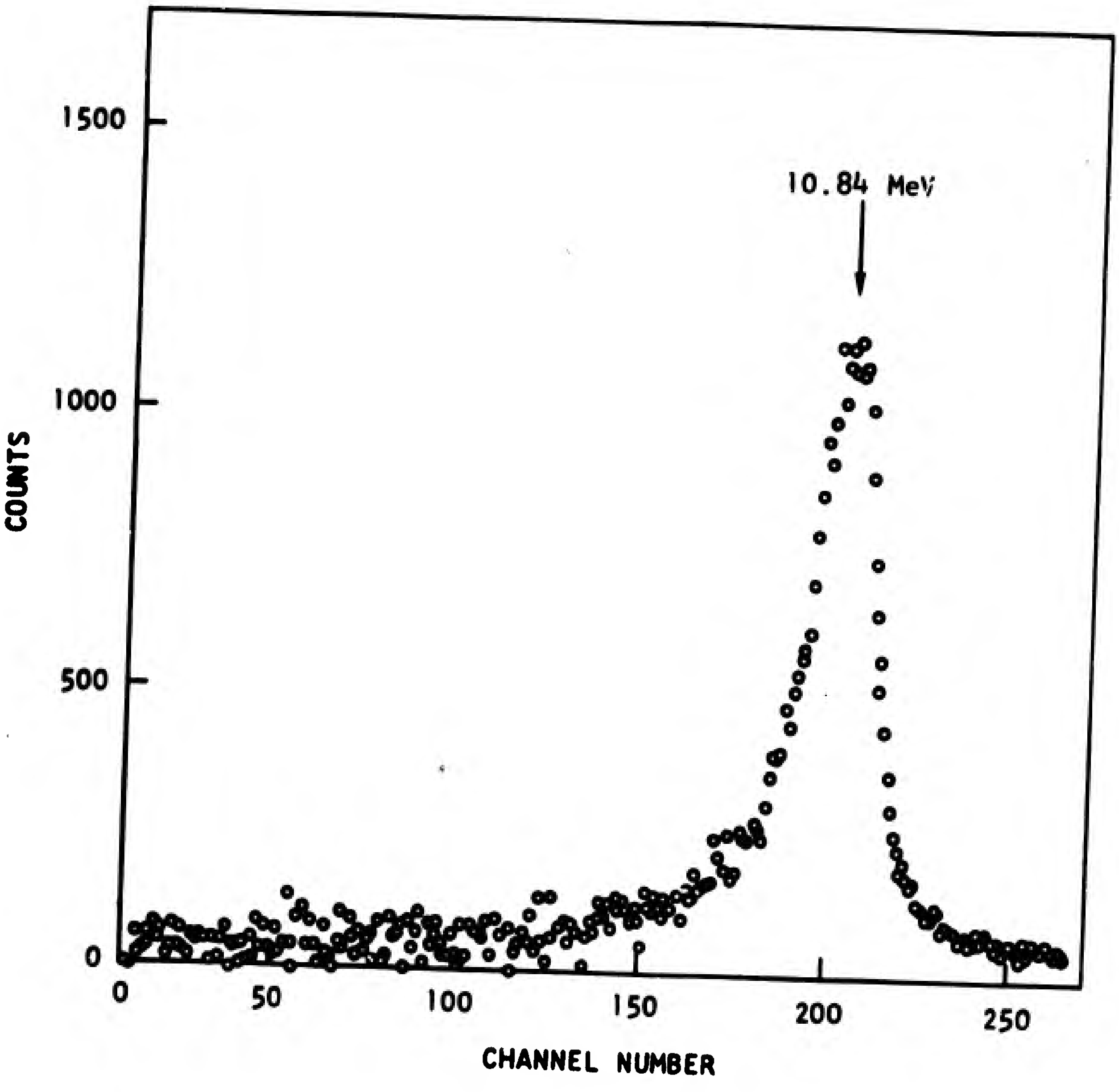

Fig. 6--Pulse-height spectrum of γ rays from the in-flight annihilation of a 10.09 MeV positron beam (bremsstrahlung has been subtracted).

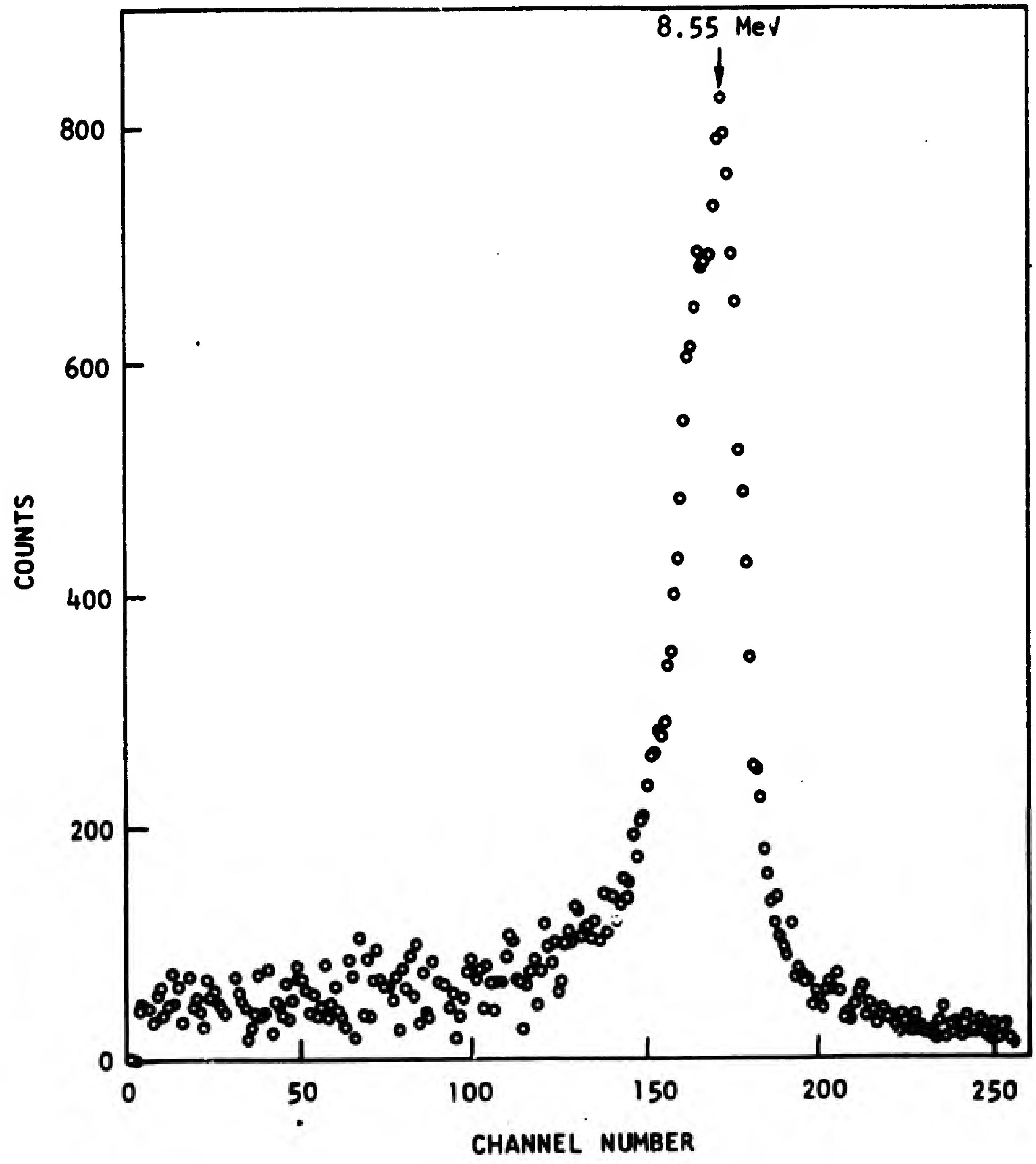

Fig. 7--Pulse-height spectrum of γ rays from the in-flight annihilation of a 7.80 MeV positron beam (bremsstrahlung has been subtracted).

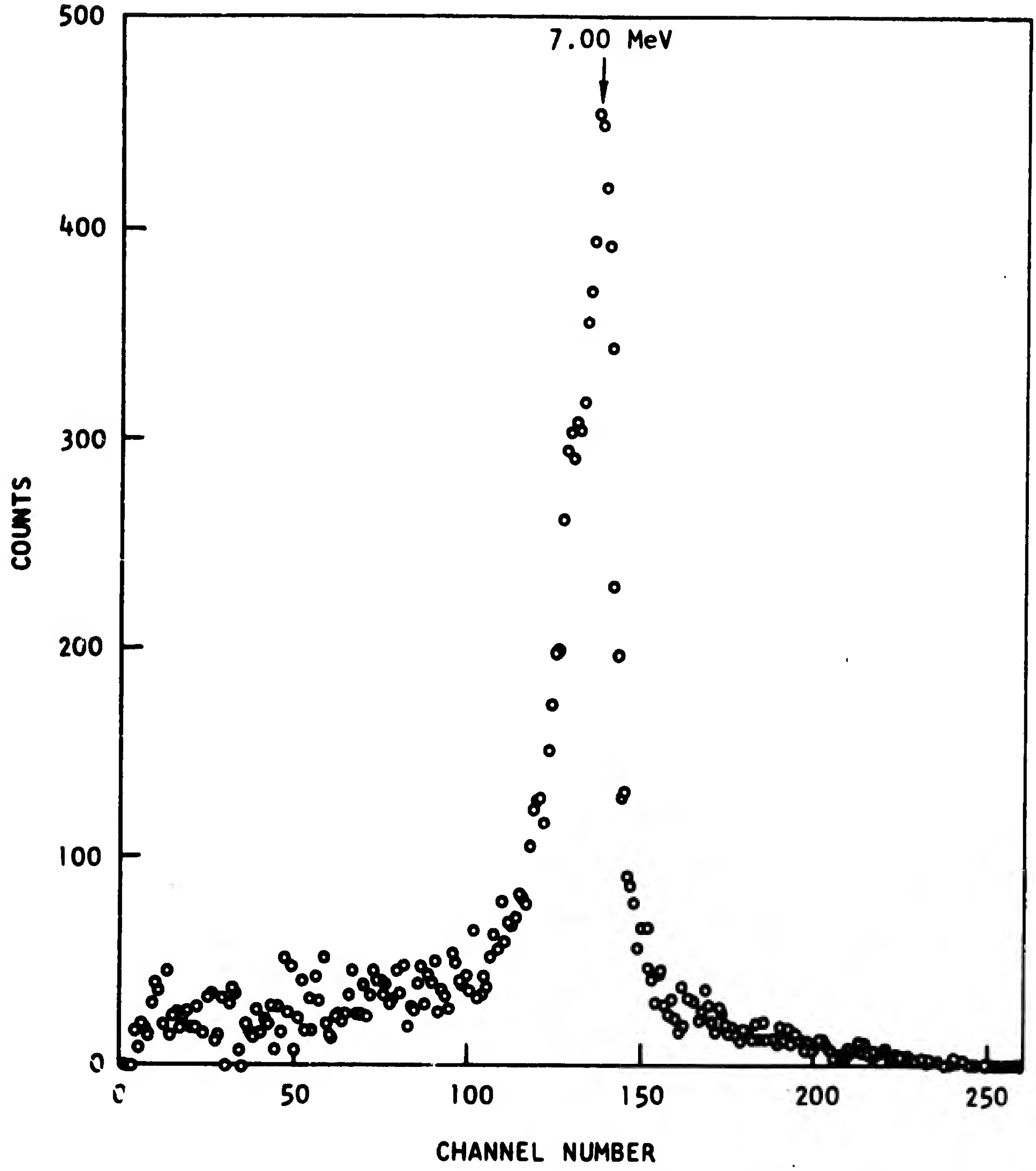

Fig. 8--Pulse-height spectrum of γ rays from the in-flight annihilation of a 6.25 MeV positron beam (bremsstrahlung has been subtracted).

by the lead collimators while the neutrons were considerably less attenuated. The spectra were subtracted yielding the pulse height spectrum shown in Fig. 9. This measurement gave the shape of the response above 2 MeV but has no value below that energy because of the inaccurate neutron subtraction.

The absolute magnitude of the response can be calculated using Eq. (1) which gives the photon flux coming from the positron source. Another method makes use of the tabulated linear attenuation coefficients(7) for NaI at the energies measured. These coefficients are known to three percent in the range of interest. The geometry of the detector and the gamma-ray sources are such that very little error is incurred as a result of gamma rays entering the front face of the crystal and passing out the sides rather than the back of the crystal. The latter method was used by NRDL when they incorporated these data into their unfolding program.

5. SHIELDING DATA

In the second part of this program several runs were made in order to obtain shielding data. On all these runs a 10 MeV photon beam was used. To do this a positron beam of total energy 9.75 MeV was tuned onto the beryllium foils in the positron annihilation system. The photons emerging from the positron annihilation system were directed at an aluminum slab which consisted of six 1-in. thick aluminum slabs placed close together. The lateral dimensions of these slabs were 36 in. x 36 in. In calculations made early in the program(3) the effect of the sides of the slabs was determined for various slab dimensions. It was shown in these calculations that the slabs chosen for this experiment would introduce no measurable error due to their finite dimensions. In other words, the slab can be considered infinite. Six inches of aluminum is equivalent to 0.95 mean free path for 10 MeV photons. Gamma-ray spectra were measured at 0°, 15° and 30° to the photon beam axis. The angles were measured from the point where the exit surface of the slab intersects the beam axis as is shown in Fig. 3. Pulse height spectra from both positrons and electrons were obtained at

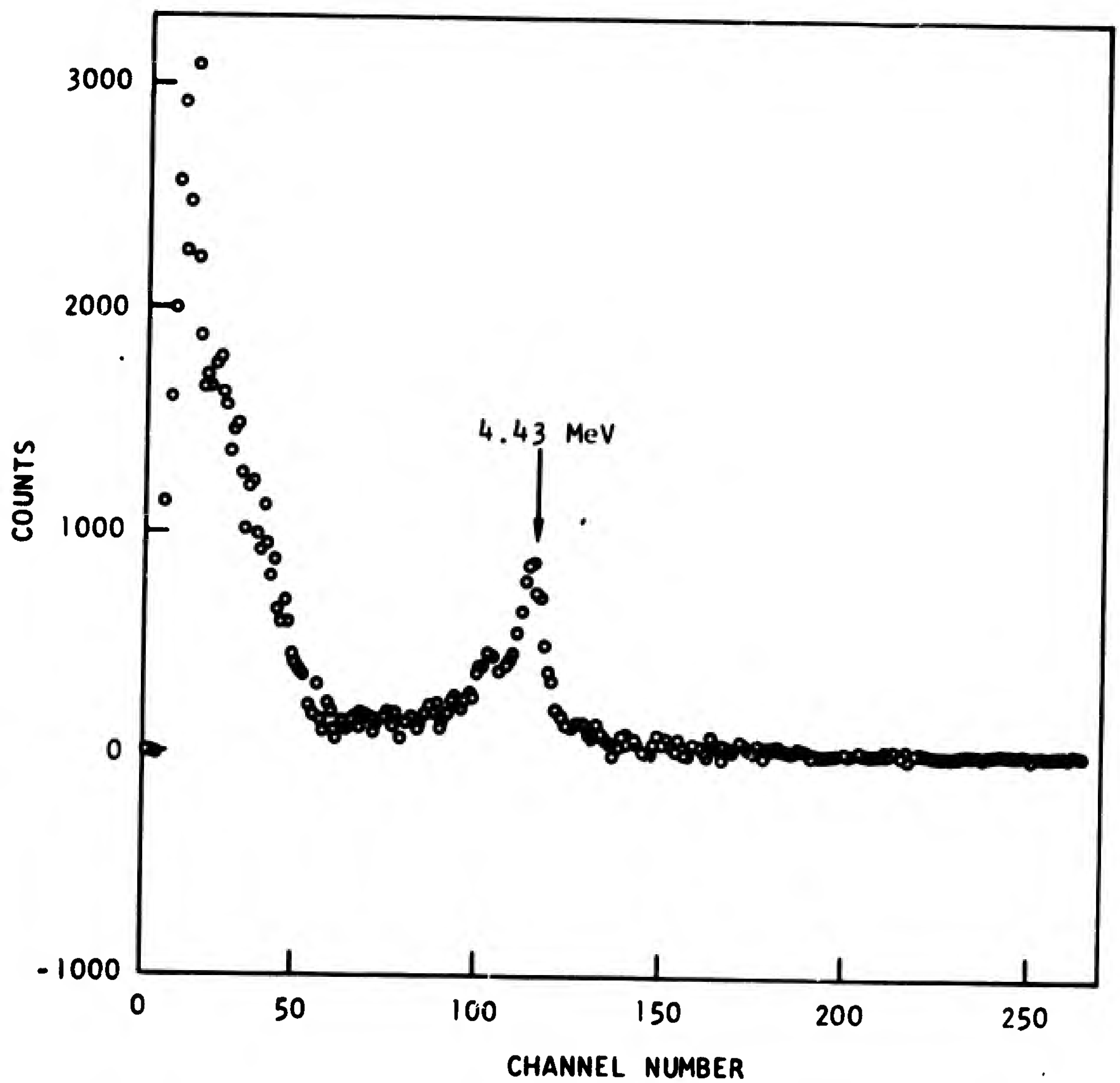

Fig. 9--Pulse-height spectrum of γ rays from a PuBe radioactive source after most of the neutron-induced γ rays have been subtracted.

each of these angles and the subtraction of bremsstrahlung was made. The resultant difference pulse height spectra are shown in Figs. 10, 11, 12.

The angular definition of the gamma-ray detection system depends on the distance from the detector to the shield. In Table 1 the distance is displayed along with the angular spread of the detector acceptances for each angle. Also listed is the corresponding solid angle subtended by the detector at the point where the photon beam axis passes through the exit face of the shield. The rather wide angular acceptance of the detection system was not a serious drawback since the form of the spectrum is not expected to vary strongly with angle except for angles very near to zero degrees. However, the penalty for obtaining a smaller angular acceptance is considerable loss in intensity. As it was, it took approximately 12 hours to obtain one spectrum, so we considered it impractical to stretch these measurements out to longer times.

Table 1

DETECTOR GEOMETRY

θ	R (inches)	$\Delta\theta$	$\Delta\Omega$ (steradians)
0°	17.5	4.9°	2.31×10^{-2}
15°	20.0	4.3°	1.77×10^{-2}
30°	17.5	4.9°	2.31×10^{-2}

The striking difference between the zero-degree spectrum and the 15° spectrum is a result of the fact that at zero degrees the detector is looking at the primary beam which is only attenuated by a factor of 0.386 before entering the detector. The distance of the detector from the slab at 15° was chosen so that the detector did not detect any portion of the primary beam. At 30° the detector was moved in closer to the shield to compensate for the loss in counting rate. Calibrations of the NaI crystal were

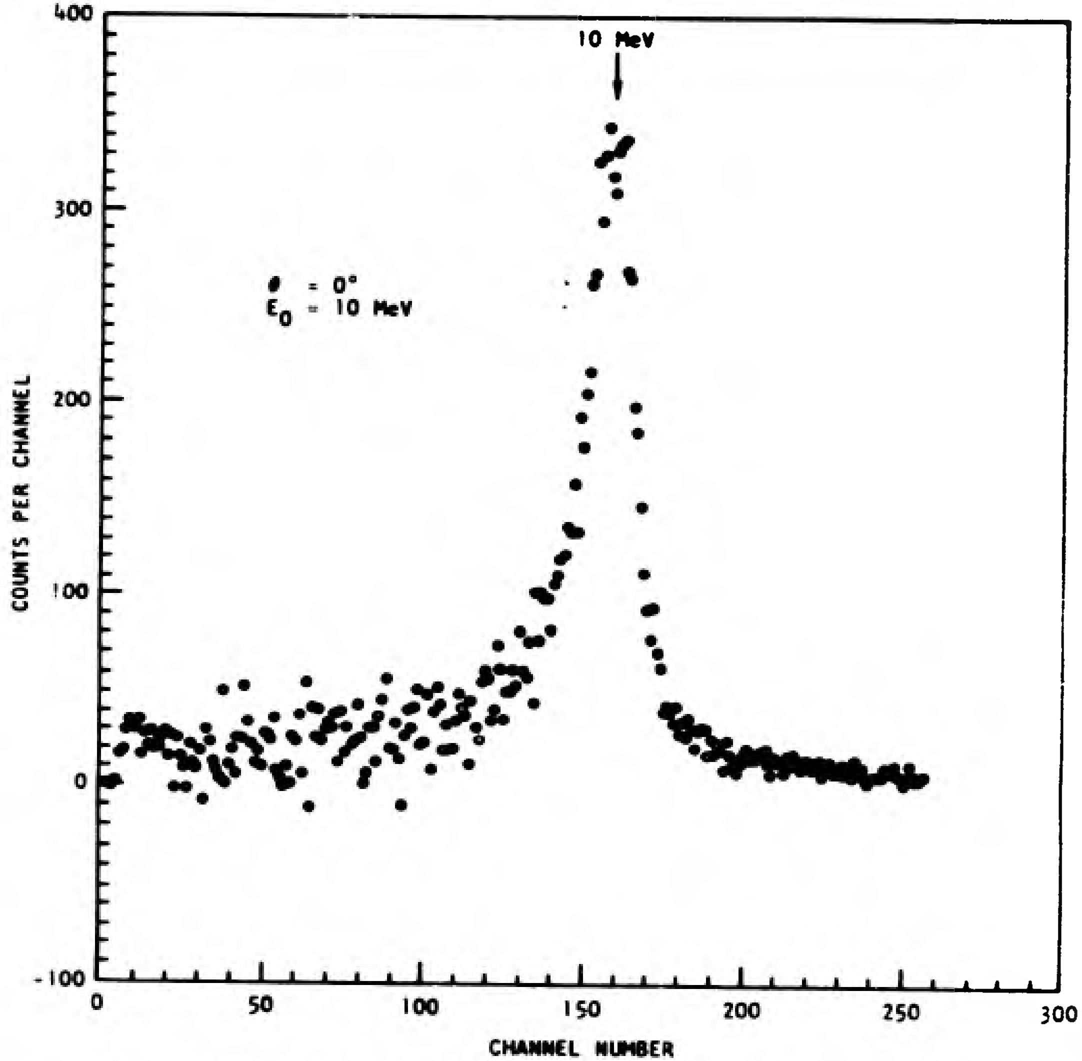

Fig. 10--Pulse-height spectrum of γ rays emerging from a slab at 0° to the 10 MeV incident photon beam

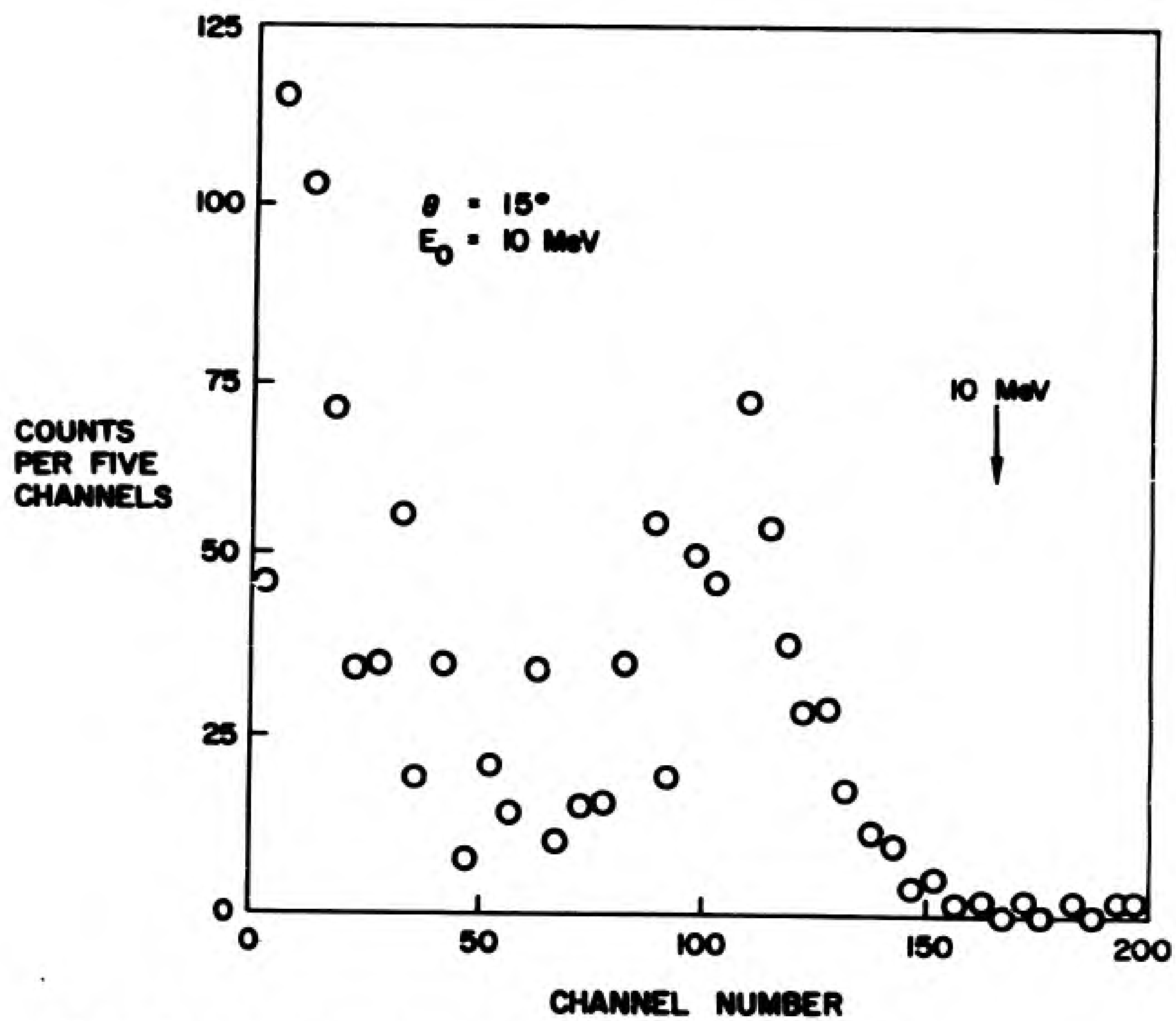

Fig. 11--Pulse-height spectrum of γ rays emerging from a slab at 15° to the 10 MeV incident photon beam

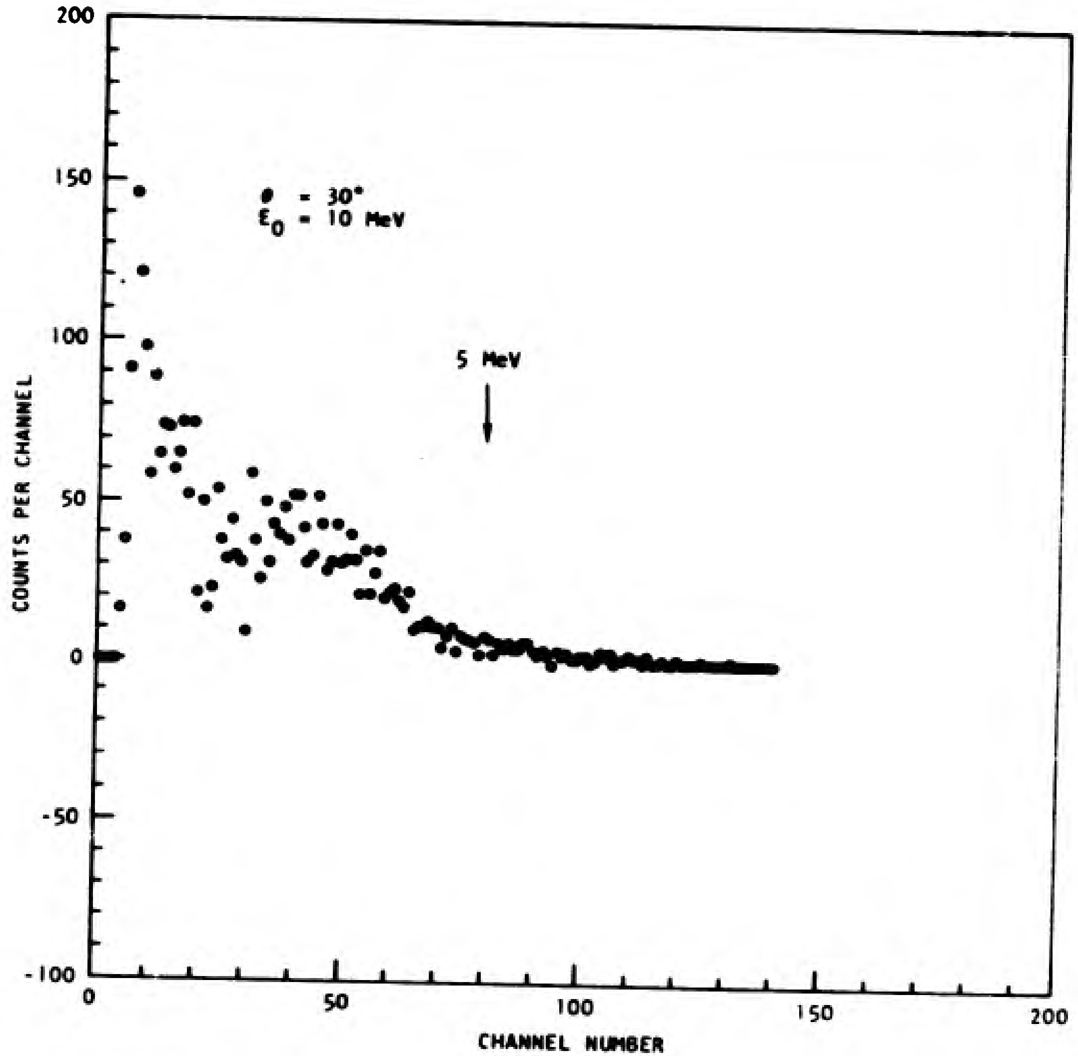

Fig. 12--Pulse-height spectrum of γ rays emerging from a slab at 30^{o} to the 10 MeV incident photon beam

made with a radioactive gamma-ray source before and after each run. During the runs yielding the spectra displayed in Figs. 10-12 there was no observed gain shift in the gamma-ray detection system.

6. DISCUSSION OF ERRORS

In the measurements of the response function and of the deep penetration of gamma rays, uncertainties can occur in several ways. One uncertainty is the energy of the incident photon beam. Another uncertainty is the accuracy with which the number of positrons and electrons entering the Faraday cup is determined. Finally there are the statistical errors associated with counting.

The spread in the energy of the gamma-ray beam is principally determined by the spread in energy of the incident positron beam. An analysis of the beam handling system yields a value for the energy spread of approximately two percent. This energy spread has also been determined for an analogous system[8] by observing the yield of 15.1 MeV resonance fluorescence gamma rays as a function of beam energy. The result of this measurement leads us to expect an energy spread of about 2.5 percent in the gamma-ray beam. The energy of the in-flight annihilation photons depends on the angle between the directions of motion of the positron and the photon. The finite size of the collimator and multiple scattering of the positron causes this angle to vary from 0°. The half-angle of the cone defined by the collimator is 0.6° which corresponds to an energy spread of 12 keV (0.12 percent) in a 10 MeV beam. From a multiple scattering theory by Moliere[9] it is expected that 96 percent of the positrons are scattered less than 2° from the initial beam direction in a 0.005 in. foil and 50 percent are scattered less than 1°. The energy difference between photons emitted at 0° and 1° to the beam is about 0.24 percent and the energy difference between photons scattered at 0° and 2° to the beam axis is about 1.2 percent. The combination of all of these uncertainties results in a total energy spread of less than 3 percent. This conclusion is confirmed by comparing the width (FWHM) of the peaks observed in the 5 in. x 6 in. NaI crystal with widths determined by Kochum and Starfelt[10] with a 5 in. x 4 in. and a 5 in. x 6 in. NaI crystal. The comparison is made in Table 2 where the first column gives the energy of the incident gamma ray, the second column gives our measured width (FWHM), and the third and fourth columns give the widths measured by Kochum and Starfelt for their two crystals.

Table 2

COMPARISON OF DETECTOR RESPONSE WIDTHS

	Crystal Size		
Energy	5 in. x 6 in.[a]	5 in. x 4 in.[b]	5 in. x 8 in.[b]
10.84	10%		
8.55	11%		
7.00	12%		
6.14		21%	13%
11.7		19%	10%

[a]This work

[b]Ref. 9

The errors associated with the current measurement are due to several sources which are treated independently since there is no correlation between them. Following are the significant correlation sources and the percentage uncertainty associated with each:

1.	Dark current	-2 percent
2.	Integrator repeatability	-0.2 percent
3.	Loss due to beam spreading	-4 percent
4.	Variation of crystal efficiency with energy	-4 percent
5.	Pile-up	-1 percent
6.	Instrument parameter measurements	-0.5 percent

These sources of uncertainty except (4) apply to all the analyses, however, (4) applies only to the integral comparison. In that method of analysis an average crystal efficiency was assumed for all energies. The RMS average of these uncertainties is 6.2 percent. The last category of uncertainty is that associated with counting random events. Statistical error is assumed to be the standard deviation and enters into the total error of each result as an independent contribution.

7. DATA ANALYSIS AND DISCUSSION

7.1 Integral Comparison

The shielding measurements described here were compared in an integral manner with calculated predictions. That is, the total number of gamma rays observed in the energy region in which the detector is sensitive was determined and compared with the total number predicted on the basis of a Monte Carlo calculation of Berger.[10] An integral comparison of this type has the advantage of providing the best possible statistical certainty with the present data. Therefore, we are able to make a meaningful quantitative comparison with the calculations. The procedure for obtaining the total number of detectable gamma rays per incident gamma ray is described below as well as the method of reducing the calculated data to correspond to the experimental situation.

To determine the number of outgoing photons per incident photon the number of incident photons must be calculated from the charge collected on the Faraday cup. That charge was calculated with Eq. 2. During the data taking runs the average current was continuously monitored and the elapsed time of the run was recorded. With these two quantities the charge was calculated independently. This latter calculation provides a good check on the integration procedure which is inherently more accurate but subject to gross mistakes. In Table 3 the charge computed from the integrator and the charge computed using the average current are displayed for both the electron and the positron runs at each angle. In the last column the

Table 3

TABULATION OF CHARGE DETERMINATIONS

Angle	Particle	Charge (Coul) Integrated	Charge (Coul) From Average Current	Difference (percent)
0°	e^{+}	6.00×10^{-8}	5.94×10^{-8}	1
	e^{-}	6.00×10^{-8}	6.81×10^{-8}	13
15°	e^{+}	2.53×10^{-7}	2.51×10^{-7}	1
	e^{-}	2.53×10^{-7}	2.61×10^{-7}	3
30°	e^{+}	9.97×10^{-7}	10.14×10^{-7}	2
	e^{-}	9.97×10^{-7}	9.40×10^{-7}	6

percentage differences between the two computations indicate that there was no procedural error made in charge integration. It also indicates that there were no long-term fluctuations in the average current and therefore that there was probably very little drift in the accelerator performance. The number of photons incident on the slab was determined for each run by using Eq. 1. This equation can be reduced to the more convenient form of Eq. 3 for 10 MeV photons by averaging over the solid angle subtended by the source collimator and by factoring in the effect of the 24-in. graphite beam hardener.

$$\text{Number of Photons} = 3.32 \times 10^{11}\ Q\ t \tag{3}$$

In Eq. 3. Q is the charge collected in Coulombs and t is the thickness of the beryllium foil in mils. The solid angles subtended by the 1-in. diameter source collimator is 2.325×10^{-4} steradians. This value was used to obtain Eq. 3 from Eq. 2. Foil thicknesses were determined by weighing the foils and measuring their dimensions. A tabulated value of the density (1.85 g/cc) was used to obtain the thickness in mils. However, Eq. 3 is independent of choice of a value of density for the beryllium since inverse density is factored into the numerical constant.

The number of gamma rays emerging from the aluminum slab in the energy interval from 600 keV to the maximum energy was estimated by a procedure indicated in Eq. 4.

$$\text{Number of Emergent } \gamma \text{ rays} = \frac{\sum_{10}^{256} N_i(\beta^+) - \sum_{10}^{256} N_i(\beta^-)}{\epsilon} \qquad (4)$$

The pulses from the positron run and the electron run were summed from channel 10 (which corresponds to 600 keV) to channel 256. The difference between these two sums was then divided by the detector efficiency, ϵ, in order to determine the total number of detectable gamma rays. The value of ϵ used in these calculations was determined from the linear attenuation coefficient for 10 MeV gamma rays passing through NaI. The error incurred by using this energy rather than averaging over the whole energy spectrum is less than 4 percent. The ratio of the number of detectable gamma rays to the number of incident gamma rays at a particular angle is determined by dividing the result of Eq. 4 by the result of Eq. 3 for that angle. Values of this ratio for the three angles at which measurements were made are listed in Table 4 under the column titled Experimental. Also listed are comparable ratios obtained from the calculations that will be described below. The error quoted on the experimental determination of each ratio is the result of approximately equal contributions from statistical errors and from experimental uncertainties described in the last section.

The calculated values displayed in Table 4 were obtained from calculations made by Martin Berger at NBS.[1] Berger calculates(as a function of angle, energy and thickness) the flux of gamma rays emerging from a thick slab of aluminum upon which is incident a monoenergetic beam of gamma rays. The outgoing gamma rays are divided into three categories, those which have undergone only one Compton scatter in the slab, those which were produced by pair production in the slab, and those which have

Table 4

COMPARISON OF COMPTON AND MULTIPLE SCATTER EVENTS

Angle	Number of Emergent Photons per Incident Photon		Exp/Theor
	Calculated[4]	Experimental	
0°	0.317	0.328 ± 0.044	1.03 ± 0.14
15°	4.28×10^{-3}	$(3.43 \pm 0.56) \times 10^{-3}$	0.80 ± 0.13
30°	2.11×10^{-3}	$(2.07 \pm 0.28) \times 10^{-3}$	0.98 ± 0.13

undergone more than one interaction in the slab. The gamma rays emerging at angle, θ, and having undergone only one Compton event in the slab will have an energy given by

$$E(\theta) = \frac{M_o C^2}{\left[1 - \cos\theta + \dfrac{M_o C^2}{E_o}\right]} \tag{5}$$

where M_o is the rest mass of the electron, C is the velocity of light, θ is the angle at which the gamma ray emerges, and E_o is the energy of the incident photon. The probability that a gamma ray will be Compton scattered through an angle θ is given by

$$P(\theta) = \left.\frac{d\sigma}{d\Omega}\right|_\theta \eta \left[\frac{e^{-\lambda_\theta t/\cos\theta} - e^{-\lambda_o t}}{\lambda_o - \lambda_\theta/\cos\theta}\right] \tag{6}$$

here $d\sigma/d\Omega_\theta$ is the differential cross section for Compton scattering evaluated at the angle, θ. This cross section was determined from the Klein-Nishina formula. The quantity, η, is the number of electrons per unit volume in the slab material, λ_o is the linear attenuation coefficient corresponding to a gamma ray of the same energy as the incident gamma ray passing through the slab material; λ_θ is the linear attenuation coefficient associated with a gamma ray passing through the slab material at the angle θ with the beam axis with its energy given by Eq. (5), and t is the thickness of the slab.

Gamma rays produced by pair production in the slab will have an energy of 511 keV. The detection system used in these experiments was sensitive down to about 600 keV so that pair production events were not observed. Multiple scatter events were accounted for by a Monte Carlo technique in which 8000 histories were obtained. In the Monte Carlo calculation the possibility of annihilation in flight and the displacement of positrons prior to annihilation have been disregarded. According to Dr. Berger these two effects are estimated to be quite small. However, more serious is the omission from the calculations of the contribution of bremsstrahlung photons produced by Compton recoil, pair- or photo-electrons. Dr. Berger predicts that for the assumed conditions this may be a 3 to 5 percent effect, which deserves further investigation. However, for the experiments performed here these effects will be small compared to the experimental uncertainties and will not impair the validity of a comparison of these calculations with the experimental results.

The results of the calculations were adjusted to correspond to the experimental geometry in order to make the comparison. In Eq. 7 the adjustment for the 0° configuration is indicated.

$$\frac{\text{No. of photons}}{\text{Incident photon}} = e^{-\lambda t} \frac{\Delta\Omega\ (\text{det. coll.})}{\Delta\Omega\ (\text{source coll.})} + (\Sigma T_m E_m + S_c)\,\Delta\Omega\ (\text{det}) \qquad (7)$$

The first term on the right gives the contribution from gamma rays that penetrate through the slab without interacting in the slab. The quantity $\Delta\Omega$ (det. Coll.) is the solid angle defined by the detector and subtended at the beryllium foil and the quantity $\Delta\Omega$ (source coll.) is the solid angle defined by the source collimator and also subtended at the beryllium foil. The attenuation of the incident beam in the slab is multiplied by the ratio of these two solid angles because the number of detectable gamma rays is limited by the detector collimator and the number of incident gamma rays is limited by the source collimator. The second term of Eq. 7 contains the contributions from the multiple scatter term ($\Sigma\, T_m E_m$) and from the single Compton scatter events (S_c). The quantity $\Delta\Omega$ (det.) is the solid angle defined by the detector and subtended at the point on the slab where the gamma-ray beam axis intersects the exit surface of the slab. The number of detectable gamma rays per incident gamma rays is calculated for angles other than 0^o, by using Eq. 8.

$$\frac{\text{No. of photons}}{\text{Incident photon}} = (\Sigma\, T_m S_m + S_c \Big|_{\theta \neq 0} \Delta\Omega(\text{det}) \qquad (8)$$

The result of adjusting Berger's calculations to the experimental geometry is displayed in Table 4 under the column headed Calculated. From Table 4 it can be seen that there is agreement between experimentally measured exit gamma-ray fluxes and the calculated gamma-ray fluxes at the three angles where measurements were made.

7.2 Spectral Comparison

Energy spectra were unfolded from the pulse height spectra measured at 0^o and 15^o to the beam axis. The unfolding was performed at USNRDL under the direction of Dr. James Ferguson. The code uses an iterative process in which sample energy spectra are repeatedly folded with the experimental response function until the resultant pulse height spectrum matches the measured pulse height spectrum within specified tolerances. The computer code is a refinement of a program written several years ago at NRDL.[11] The resultant energy spectra are displayed in Figs. 13 and 14. The experimental response function did not contain a measurement below 4.43 MeV. This omission seriously affected the validity of the unfolding process below approximately 3.0 MeV. As a result it was not possible to unfold the pulse height spectra measured at 30^o, since there is not a significant number of gamma rays with energies above 3 MeV emerging at this angle.

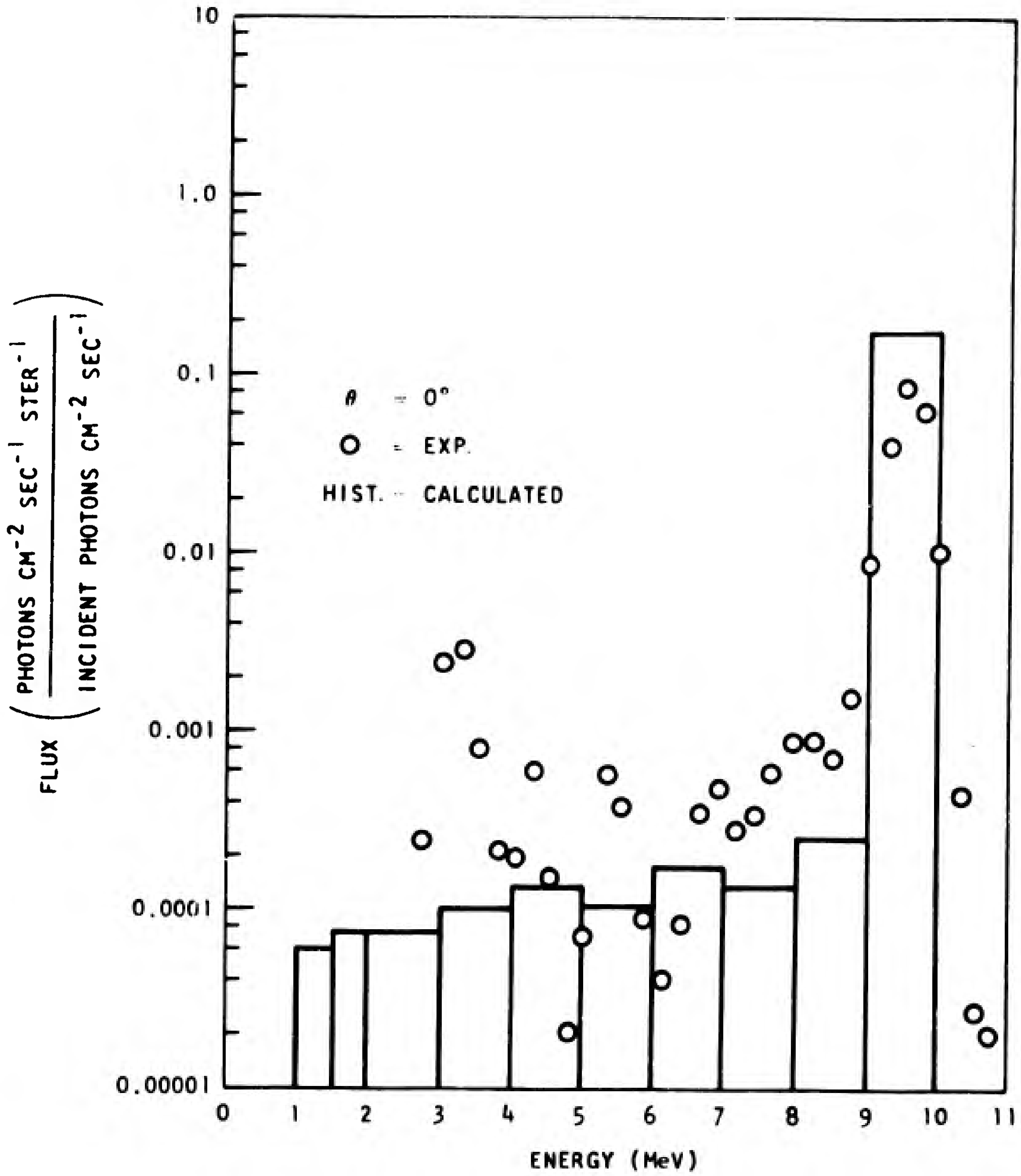

Fig. 13--Energy spectrum of γ rays emerging from a slab at 0° to the 10 MeV incident photon beam

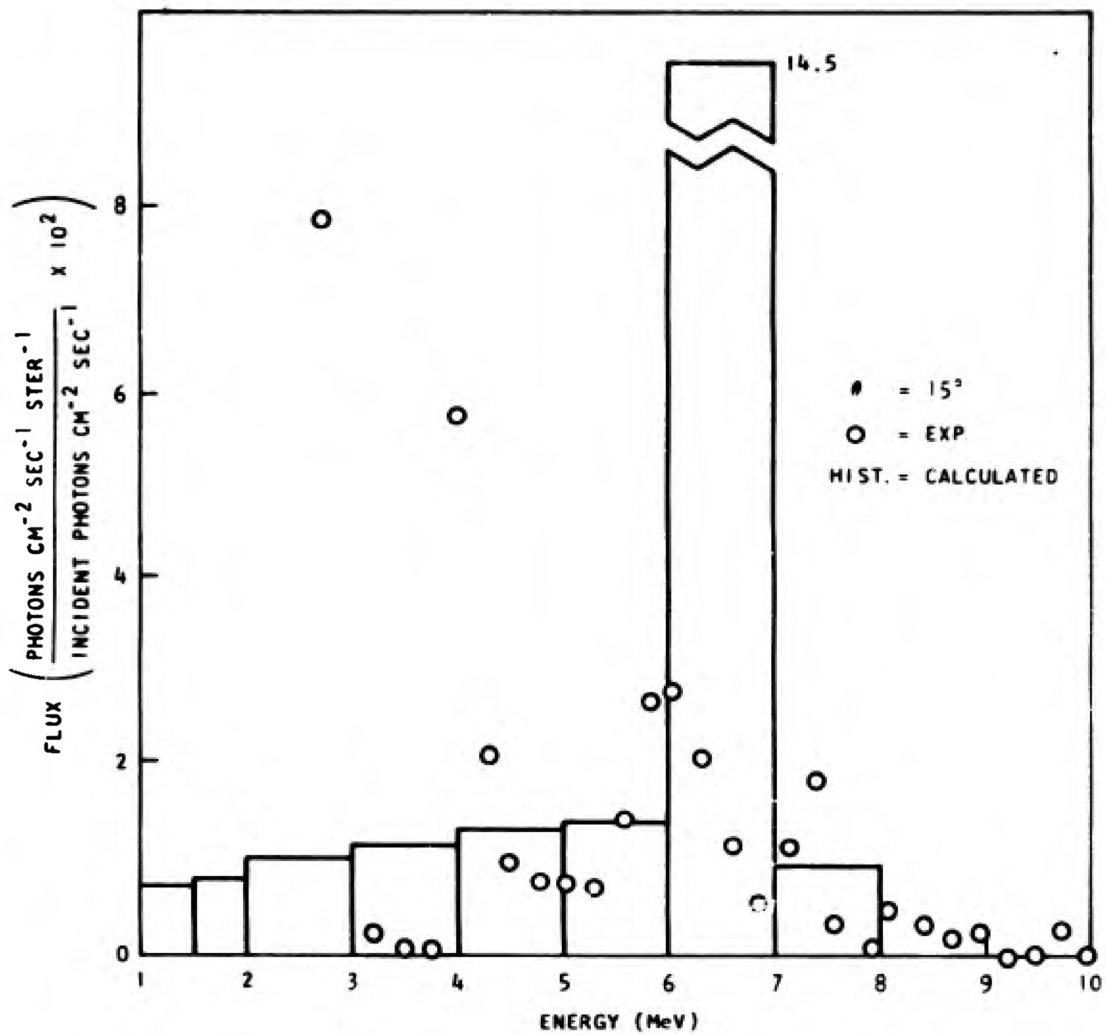

Fig. 14--Energy spectrum of γ rays emerging from a slab at 15° to the 10 MeV incident photon beam

Plotted with the experimental energy spectra in Figs. 13 and 14 are the energy spectra (histograms) calculated by Berger.[1] At 0° there is agreement between the calculated and measured spectra. At 15° the agreement is poor. The lack of agreement is primarily due to uncertainties introduced by the unfolding process. Particularly the erratic behavior at the low energy end is attributable to the lack of response information in this region. However, the detector response at higher energies is fairly well established, yet the experimental spectra does not indicate the presence of a large single Compton scatter component.

8. CONCLUSIONS

Pulse height spectra of gamma rays emitted from a six-inch thick slab of aluminum have been measured at 0°, 15° and 30° to a beam of 10 MeV photons normally incident on the slab. The total number of photons emitted in the energy range from 0.6 to 10 MeV per incident photon and per unit solid angle was calculated for each of these spectra. A similar number was computed from Monte Carlo calculation of photon transport. These quantities are compared in Table 4 and found to agree within experimental certainty. Energy spectra were unfolded from the pulse height spectra measured at 0° and 15°. A response function measured in this program was used along with a computer code developed at NRDL to do the unfolding. These energy spectra are compared in Figs. 13 and 14 with the energy spectra calculated by the Monte Carlo technique. There is agreement at 0° but not at 15°. The disagreement at 15° is primarily due to inadequacies in the unfolding process. However, there appears to be a much smaller single Compton component than is predicted. Further experimental work is required in order to make a conclusive remark concerning the apparent discrepancy.

REFERENCES

1. M. J. Berger, Private Communication with D. F. Herring, General Atomic, Jan. 4, 1966.

2. R. E. Sund, R. B. Walton, N. J. Norris and M. H. MacGregor, Nucl. Instr. and Methods, 27 109 (1964).

3. D. E. Groce, J. A. Lonergan, "Gamma-Ray Shielding Studies," General Atomic Report GACD-6944 (4-30-66).

4. W. Heitler, "The Quantum Theory of Radiation," (Oxford University Press, New York, 1954), 3rd ed.

5. F. D. Seward, C. R. Hatcher and S. C. Fultz, Phys. Rev. 121, 605 (1961).

6. H. W. Kendall and M. Deutsch, Phys. Rev. 101, 20 (1956).

7. G. W. Grodstein, National Bureau of Standards Circular No. 583 (U. S. Government Printing Office, Washington, D. C., 1957).

8. R. B. Walton and R. E. Sund, "Basic Photonuclear Research," General Atomic Report GA-6982, Feb. 1966.

9. G. Molieri, Z Naturforsch, 34, 78 (1948).

10. J. Kochum and N. Starfelt, Nucl. Inst. and Meth., 4, 171 (1959).

11. C. V. Smith and N. E. Scofield, USNRDL-TR-829 (1965).